Research and Reviews: Journal of Material Sciences e-ISSN: 2321-6212

A Comparative Study of Spin Magnetic Moment, Spin Polarization and Curie Temperature of Heusler Type Compounds $(A_{2-x-y}Z_y)MnZ$ (A=Ni, Pd, Pt and Z=Sb, Sn)

M Shahjahan*, SC Roy, MJ Sadique

Department of Physics, University of Dhaka, Dhaka, Bangladesh

Research Article

Received: 09-December-2019, Manuscript No. JOMS-19-5420; **Editor assigned:** 12-December-2019, Pre QC No. JOMS-19-5420(PQ); **Reviewed:** 26-December-2019, QC No. JOMS-19-5420; **Revised:** 28-July-2022, QI No. JOMS-19-5420; Manuscript No. JOMS-19-5420(R); **Published:** 25-August-2022, DOI: 10.4172/2321-6212.10.7.007.

***For Correspondence:**
M Shahjahan, Department of Physics, University of Dhaka, Dhaka, Bangladesh

E-mail: mjahan@du.ac.bd

Keywords: Density; Curie temperature; Spin polarization; Magnetic moment

ABSTRACT

The Heusler type compounds $(A_{2-x-y}Z_y)MnZ$ (A=Ni, Pd, Pt; Z=Sb, Sn; x=1, 0; and y=0, antisite defects of Z atoms) are investigated to under-stand the induced magnetic properties. The structural phases $C1_b$ type half Heusler (x=1, y=0) compounds AMnZ and the corresponding $L2_1$ type full Heusler (x=y=0) compounds A_2MnZ and some disordered compounds $(A_{1-y}Z_y)MnZ$ and $(A_{2-y}Z_y)MnZ$ were calculated using the Korringa-Kohn- Rostoker Green's function method. The antisite doping of 1% (5%) Sb re-tain (suppressed) the half metallicity at $(Ni_{1-y}Sb_y)MnSb$, whereas the other compounds were found to be gapless in both spin directions. Density of states at the fermi level exhibit the explicit spin polarization of the compounds. The net magnetic moments of the compounds are closer in their values, wherein the manganese atom is responsible for the major contribution of magnetic moments, which is enough larger than the partial moment of other constituents. The Curie Temperature (TC) of the ordered ferromagnetic compounds was estimated using the mean field approximation. The TC higher than the room temperature was found for the ordered compounds, except for the cases of Pt_2MnSb and Pt_2MnSn. No literature value of TC is reported yet for these two compounds. Calculated spin moments and TC agree well with the available experimental results.

INTRODUCTION

The Heusler type intermetallic compounds $(A_{2-x-y}Z_y)MnZ$ (A=Ni, Pd, Pt and Z=Sb, Sn) have drawn attention to the metallurgist because of their promising technological applications. The collinear magnetic and half metallic

behavior with noticeably high Curie temperature (TC) as well as magneto-mechanical properties made these materials unique. The magnetic shape memory effect, large strain-induced changes in the magnetization and field induced super elasticity are also found in Heusler materials. It is desirable to have a magnetic shape memory alloy with the TC higher than the Room Temperature (RT). The saturation magnetic moment and TC are very much dependent on the composition of Heusler compounds. Since Heusler materials exhibit most of the properties of metals, but have the structure of an ordered like compounds, therefore several different magnetic exchange mechanisms play role to them. There are two major classes of Heusler materials with compositions AMnZ (x=1, y=0) treated as Half Heusler (HH) compounds and A_2MnZ (x=y=0) termed as Full Heusler (FH) compounds, where A (Ni, Pd, Pt) and Mn are transition metal (TM) atoms and Z (Sb, Sn) denotes primary group atom [1].

Heusler compounds were first studied in 1903 by Heusler, who reported that it was possible to make Ferromagnetic (FM) compounds from the non-FM constituents. He found the FM property in many of the compounds, although neither of the constituents were FM at all. Since then these alloys have been studied theoretically and experimentally to predict new featured magnetic materials. In fact, the magnetic properties of these compounds are sensitive to the local geometry, chemical composition and to the ordering of the manganese atoms in the Face Centered Cubic (FCC) sublattices. In 1983, de Groot and his coworkers have shown in their revolutionary letter that these materials belong to a novel class half metals, which has been since then studied rigorously. By this time, many other interesting properties of Heusler compounds have been pointed out by some other research groups [2].

Recently, Luo group investigated the electronic structures and magnetic properties of the HH compounds and predicted NiCrAl, NiCrGa and NiCrIn as possible half metals with an energy gap in the minority spin and a full spin polarization at the Fermi level. Kaneko group had measured the pressure effect on the Curie point of FH compounds Ni_2MnSn and Ni_2MnSb with the pressure coefficient as 1.6×10^{-3} $kbar^{-1}$ and 9×10^{-3} $kbar^{-1}$, respectively. In the advent of spintronics, these materials become attractive because the half metallic behavior of these materials are of prime interest to the metallurgist.

In spintronic devices, spin-dependent electronic transport can be used to encode information by changing finite resistance through these magnetic half metals. These devices show increased integration densities, non volatility of information, high speed data processing, and reduced energy consumption rather than conventional semiconductor electronics. Strictly speaking, such type of transport with spin degrees of freedom have superseded the traditional semiconductor technologies [3].

Structurally, the HH and FH compounds belong to the C_{1b} and $L2_1$ type phases, respectively with the FCC sub-lattices in the unit cell. These materials can be FM, ferrimagnetic, antiferromagnetic and nonmagnetic depending on the conduction electron concentration and chemical bonding. Therefore, greater interest have grown for in depth study on the magnetic interactions present in these materials. In most of the Heusler compounds, Mn is the primary moment carrying atom. The presence of localized spins (magnetic ions) of the d electrons of A and Mn atoms, an indirect RKKY (Ruderman-Kittel-Kasuya-Yosida) type exchange interaction plays role behind the origin of magnetic

anisotropy of the system. The exchange mediated by electron or hole states is obtained from the hybridized states by second-order perturbation theory [4].

In this article, we are motivated to realize the FM and half metallic treatment in Heusler type disordered compounds. A comparative study of electronic and spin polarized properties of the Heusler type twenty four compounds ($A_{2-x-yzy}$) MnZ (A=Ni, Pd, Pt; Z=Sb, Sn; x=1, 0; and y=0, antisite defects of Z atoms) are investigated to explain the induced magnetic properties. The antisite doping of 1% (5%) Sb retain (suppressed) the half metallicity at ($Ni_{1-y}Sb_y$) MnSb.

The magnetic moments and spin polarizations of the Heusler type compounds are calculated, whereas the TC is estimated only for the ordered Heusler materials. Despite closeness of the experimental magnetic moments for the ordered systems, their Curie temperatures appeared to differ strongly. Moreover, spin-resolved electronic Density of States (DOS) are calculated to seek the underlying reasons for the induced partial moments, polarity of moments and spin polarized properties of the Heusler type compounds [5].

Computational details

The layout of the article is organised as follows. The computational framework is briefly outlined in section 2. The results and discussion part is subsectioned into three pats, namely magnetic moments, Curie temperature, and spin-resolved electronic density of states, which are explained in details in section 3. The comparison of the calculated values with the reported experimental results. The moments of the disordered systems are assembled, whereas their DOS. Finally, the concluded remarks on the presented results are outlined in section 4 (Figures 1 and 2).

Figure 1. Unit cell of half Heusler (Ni, Pd, Pt) implies transition metal atom and Z (Sb, Sn) signifies primary (p) block atom.

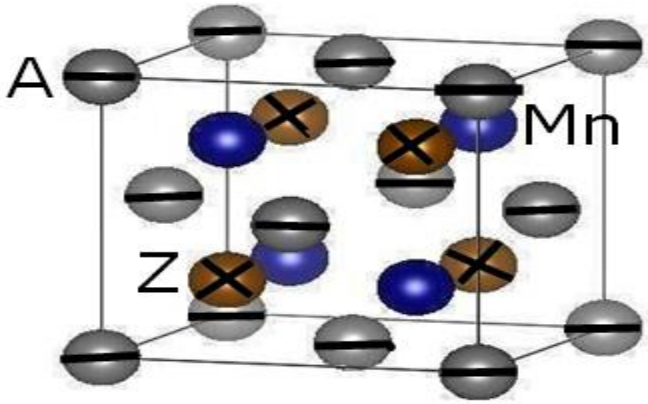

Figure 2. Unit cell of full Heusler crystal structures with three and four atoms in the formula unit, respectively. Here A (Ni, Pd, Pt) implies transition metal atom and Z (Sb, Sn) signifies primary (p) block atom.

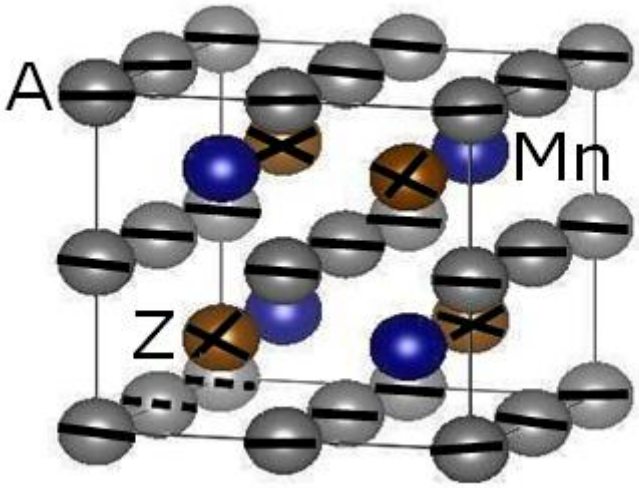

Spin polarization and collinear magnetic properties of Heusler type compounds were calculated using the KKR-Green's function method, where two magnetic states were calculated for two different spin orientations. The calculations were carried out within the formalism of scalar relativistic approximation by neglecting spin-orbit interactions. The generalized gradient approximation was used for the exchange correlation functional of the potential scheme. The Muffin-Tin (MT) potential approximation was used, where the MT radius was selected such that the potential spheres are mildly touched, but non-overlaped each other. The Mean Field Approximation (MFA) was used to calculate the TC. In total 328 k points of the first Brillouin Zone (BZ) were included to perform the BZ integration. The compounds were taken to be crystallized in the FCC structure. The L21 phase of FH compounds A_2MnZ, where two atomic coordinates of A atoms are (0.25, 0.25, 0.25), (0.75, 0.75, 0.75), coordinates of Mn and Z atoms are Mn(0.5, 0.5, 0.5) and Z(0,0,0). For the case of C_1b phase of HH compounds AMnZ, one of the two sites of A atoms becomes empty. The accuracy of the C_1b phase calculations was assured by filling the one vacant site with a dummy atom having zero nuclear charge. Lattice relaxation was neglected in the present calculation, which would further lower the total energy. The experimental Lattice Parameters (LP) were used for the four HH and one FH Ni_2MnSb compounds. Theoretical LP were used for two FH compounds Pd_2MnSb and Pt_2MnSn. The LP of the FH compound Pt_2MnSb was estimated using the energy minimization technique, which is lacking of any experimental or theoretical values in the literature. The LP of the ordered compounds are directly used for the calculation of disordered compounds. The software package Machikaneyama 2002 is used for the numerical computations [6].

RESULTS

The material diplatinum manganese antimonide, Pt_2MnSb is regarded as a media for high density magnetooptic memory systems. Its LP was estimated using the energy minimization scheme, as shown in Figure 3, where the calculated ground state energy is plotted with respect to the LP. The parameter against minimum energy is opted

from the graph, as indicated by the dashed lines. Then using the calculated optimized LP, its collinear magnetic and electronic properties have been calculated. The investigated material is deemed FM and therefore its magnetic critical temperature is calculated in comparison to the ground state energy of the corresponding Disordered Local Moment (DLM) state. As far as we know, there is no explicit report on the value of its LP neither experimentally nor theoretically in the literature. This material exhibits FM properties with low TC. Its FM stability can be explained by the RKKY type exchange interactions, which is schematically digramed in Figure 4. The non-localized conduction electron's spin interact with the localized inner d electron spins and thus creating a linear correlation energy between the spins. The d electron spins are therefore aligned through this interaction and thereby stabilizes the FM state (Figures 3 and 4).

Figure 3. Calculated lattice parameter of a full Heusler compound Pt_2MnSb using energy minimization technique.

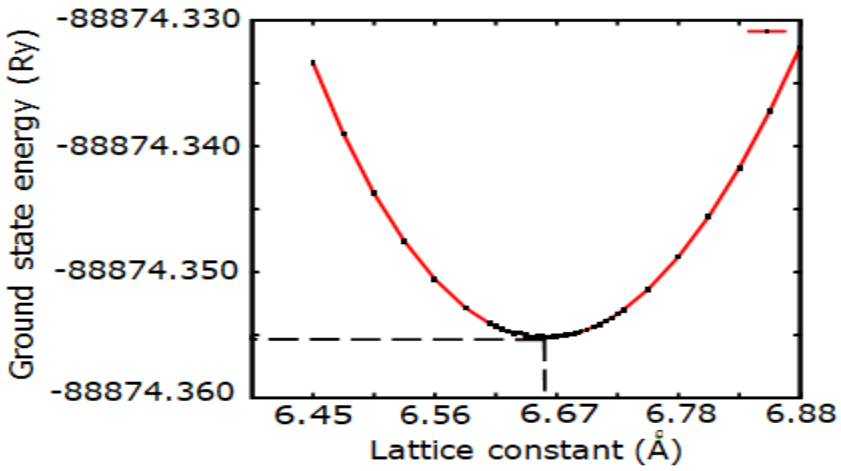

Figure 4. Schematic diagram of RKKY type exchange interaction, which makes spin state stable.

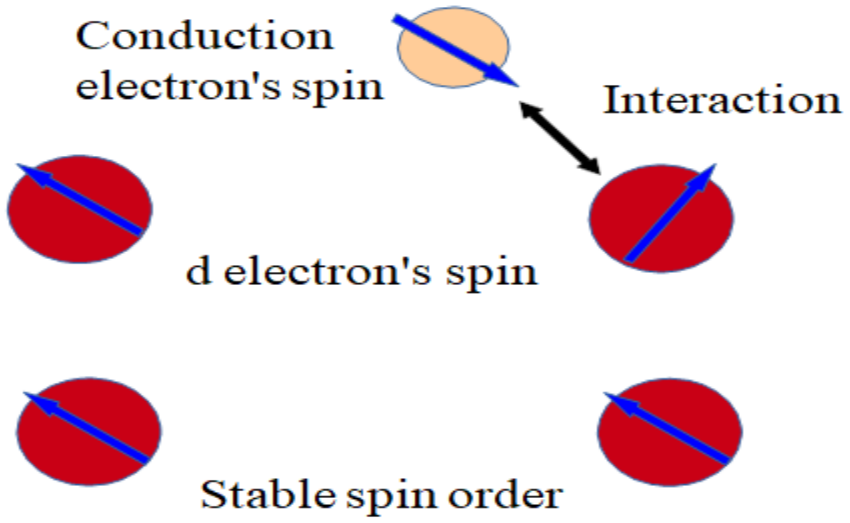

Magnetic moments

The magnetic moment represents the magnetic strength and orientation of a magnetic material resulting from the motion of electrons in atoms, or the spin of the electrons. The saturated magnetic moments are calculated for four (Table 1).

Table 1. Lattice constant (a), partial and total magnetic moments and Curie temperature of the half Heusler compounds $(A_{2-x-y}Z_y)MnZ$ (x=1, y=0). TM^{calc} (TM^{expt}) represents the calculated (experimental) values of the total moment. The ΔE represents the energy difference between DLM and FM states. T_{calc} (T_{expt}) represents the calculated (experimental) values of curie temperature. Here A and Z indicate the first and third atoms of the compounds AMnZ.

Materials	a (˚A)	A (μ_B/atom)	Mn (μ_B/atom)	Z (μ_B/atom)	Vacancy (μ_B/atom)	Tm^{calc} (μ_B/cell)	Tm^{expt} (μ_B/cell)	ΔE (mRy)	TC^{calc} (K)	TC^{expt} (K)
NiMnSb	5.92	0.219	3.871	-0.11	0.008	4.001	3.85	11.6	1221	730
PdMnSb	6.25	0.078	4.189	-0.14	0.008	4.144	3.95	8.6	905	500
PtMnSb	6.21	0.096	4.091	-0.113	0.008	4.089	3.97	8.9	937	582
PtMnSn	6.264	0.049	4.082	-0.131	0.008	3.955	3.42	3	316	354

HH compounds namely, NiMnSb, PtMnSb, PdMnSb, and PtMnSn and eight HH type compounds $(A_{1-y}Z_y)MnZ$ (y=0.01, 0.05). The FM calculations were carried out for the compounds, where the saturated magnetic moment of each compound is found to be the sum of the local spin moments of the constituent atoms. The spin magnetic moment of an electron, an intrinsic property, is approximately one Bohr magneton, 1 μ_B. The spin magnetic moments of the constituent atoms are very low in strength compare to the spin magnetic moment of Mn atom. However, in NiMnSb, Mn site contains unoccupied minority bands, whereas Ni site contains fully occupied bands in both spin polarization. As a result, the magnetic moment of the compound is localized at the Mn site. Evidently, the net magnetic moment of the materials are mainly due to the spin moment at Mn site. The cation sites A and Mn in the formula AMnZ provide positive moments, whereas the Sb and Sn atoms at the Z site provide negative moments. In NiMnSb, PdMnSb and PtMnSb there are 22 valance electrons in each of the compounds and 21 valence electrons in PtMnSn. These materials are shown by Galanakis and others to follow the moment rule $M_t=Z_t-18$, where Mt is total magnetic moment and Z_t is the total number of valance electrons. The estimation of the magnetic moment for NiMnSb and PtMnSb exactly agree with this rule, since the calculated values of moment are almost equal to 4 μ_B. Calculated total moment of the compounds is compared with the experimental results determined by van Engen and others. Calculated values of net moment are quite closer to the measured values. The induced moments at vacancy and Z_y sites are negligible. The Anion site (Z) moments are antiparallel to the moments at cation sites [7-11].

In addition to the HH compounds, the present work consists of four FH compounds such as Ni_2MnSb, Pd_2MnSb, Pt_2MnSb and Pt_2MnSn and eight FH type compounds $(A_{2-y}Z_y)MnZ$ (y=0.01, 0.05). The partial moments of the constituent atoms and the total moment of the compounds are listed (Table 2).

Table 2. Site projected partial moments and total magnetic moments per unit cell of the half Heusler type compounds $(A_{2-x-y}Z_y)MnZ$ (x=1, y=0.01, 0.05). Z_y is the antisite doping at 1% and 5% atomic concentration of Z atoms. TM^{calc} represents the calculated values of the total moment. Here A and Z indicate the first and third atoms of the compounds $(A_{1y}Z_y)MnZ$.

Materials	Z_y (μ_B/atom)	A (μ_B/atom)	Mn (μ_B/atom)	Z (μ_B/atom)	Vacancy (μ_B/atom)	Tmcalc (μ_B/cell)
$(Ni_{0.99}Sb_{0.01})MnSb$	0.013	0.224	3.864	-0.09	0.008	4.049
$(Ni_{0.95}Sb_{0.05})MnSb$	0.013	0.298	3.908	-0.053	0.01	4.188
$(Pd_{0.99}Sb_{0.01})MnSb$	0.016	0.151	4.176	-0.134	0.007	4.179
$(Pd_{0.95}Sb_{0.05})MnSb$	0.02	0.179	4.175	-0.098	0.011	4.265
$(Pt_{0.99}Sb_{0.01})MnSb$	0.017	0.157	4.084	-0.123	0.008	4.096
$(Pt_{0.95}Sb_{0.05})MnSb$	0.029	0.198	4.108	-0.079	0.014	4.246
$(Pt_{0.99}Sn_{0.01})MnSn$	-0.047	0.125	4.143	-0.134	-0.011	3.996
$(Pt_{0.99}Sn_{0.01})MnSn$	-0.046	0.125	4.12	-0.131	-0.01	3.976

Similar to the HH compounds, the magnetic moments of the FH compounds are mainly due to the contribution of the spin magnetic moment of Mn atom. It has been verified by neutron scattering experiment that the magnetic moment of $L2_1$ type Heusler compounds resides mainly on the Mn site. Kubler and others have explained that the origin of the magnetic moment is the localized nature of the Mn atoms within the compounds. However, a general rule for magnetic moment in the FH compounds can be expressed as $Mt=Z_t-24$, where again Mt is the net magnetic moment and Z_t is the total number of valance electrons. The Ni_2MnSb, Pd_2MnSb, and Pt_2MnSb have each 32 valance electrons and Pt_2MnSn has 31 valance electrons.

Therefore, the moment rule for the cases of 32 and 31 valence electrons then predicts the value of moment to be 8 μ_B and 7 μ_B, respectively. But the calculated magnetic moments retain in the range 4 μ_B~4.5 μ_B. This fact can be explained as the paramagnetic effect of the Ni, Pd and Pt atoms at position A in the systems A_2MnZ. Due to their paramagnetic nature, these atoms fail to produce large amount of spin moments and consequently the net magnetic moment is much lower than the value predicted by the moment rule. Besides, the d electrons of Mn are itinerant, which originates the localization nature of d electron wavefunctions and the spin-down electrons are almost excluded from the Mn site. The induced moments, at Z and Z_y sites are parallel, which together oppositely oriented to the moments of cation sites [12-17]

Curie temperature

The curie temperature is the critical point at which the magnetic moments change direction randomly and the material loses its magnetic properties. The resulting spin state of the paramagnetic material is regarded as the DLM state. Consequently, the energy difference ΔE between the FM and DLM states is calculated, which is the karnel parameter to estimate TC. The expression $TC=(2\Delta E)/(3k_B)$ is used to estimate the critical temperature of the Heusler compounds, where kB is the Boltzmann constant. The estimated TC with the available experimental values. Hames and Crangle have reported the experimental TC for the PtMnSb to be 575 K and 330 K for the PtMnSn, which are closer to the values of the present calculation. The MFA often overestimates TC in comparison to the experimental results, whereas the estimated TC for PtMnSn is in good agreement with the experiments. The reason behind the overestimation is that the framework of MFA does not include abruptness of spin within the compounds. However, the Rusz group have reported that the TC for NiMnSb to be as high as 1106 K. Their calculation closely concur with the presented result for the same compound. In addition, the estimated TC of the compounds AMnZ (x=1, y=0) is found higher than the RT. Hich originates the localization nature of d electron wavefunctions and the spin-down electrons are almost excluded from the Mn site. The induced moments, at Z and Z_y sites are parallel, which together oppositely oriented to the moments of cation sites (Table 3) [18].

Table 3. Lattice constant (a), partial and total magnetic moments and Curie temperature of the full Heusler compounds $(A_{2-x-y}Zy)MnZ$ (x=y=0). TM^{calc} (TM^{expt}) represents the calculated (experimental) values of the total moment. The ΔE represents the energy difference between DLM and FM states. T^{calc} (T^{expt}) represents the calculated (experimental) values of Curie temperature. Here A^+ and A^{++} indicate the two atomic sites of A atoms in the full Heusler compounds A_2MnZ, where the letter Z indicates the third atom of the compounds.

Materials	a (˚A)	A^+ (μB/atom)	A^{++} (μB/atom)	Mn (μB/atom)	Z (μB/atom)	Tm^{calc} (μB/cell)	Tm^{expt} (μB/cell)	ΔE (mRy)	TC^{calc} (K)	TC^{expt} (K)
Ni_2MnSb	6.001	0.154	0.154	3.691	-0.044	3.968	-	4.1	432	334
Pd_2MnSb	6.424	0.077	0.077	4.187	-0.042	4.308	4.4	3.4	358	247
Pt_2MnSb	6.66	0.127	0.127	4.313	-0.008	4.592	-	0.4	42	
Pt_2MnSn	6.46	0.09	0.09	4.103	-0.023	4.264	-	1,7	179	

Table 4. Site projected partial moments and total magnetic moments per unit cell of the full Heusler type compounds $(A_{2-x-y}Z_y)$ MnZ (x=0, y=0.01, 0.05). Z_y is the antisite doping at 1% and 5% atomic concentrations of Z atoms. TM^{calc} represents the calculated values of the total moment. Here A^+ and A^{++} indicate the two atomic sites of A atoms in the compounds $(A_{2-y}Z_y)$ MnZ, where the letter Z indicates the third atom of the compounds.

Materials	Z_y (μB/atom)	A^+ (μB/atom)	A^{++} (μB/atom)	Mn (μB/atom)	Z (μB/atom)	Tm^{calc} (μB/cell)
$(Ni_{1.99}Sb_{0.01})MnSb$	-0.025	0.182	0.182	3.675	-0.058	3.942
$(Ni_{1.95}Sb_{0.05})MnSb$	-0.028	0.2	0.203	3.661	-0.051	3.951
$(Pd_{1.99}Sb_{0.01})MnSb$	-0.048	0.144	0.144	4.219	-0.045	4.364

$(Pd_{1.95}Sb_{0.05})MnSb$	-0.055	0.138	0.138	4.189	-0.047	4.319
$(Pt_{1.99}Sb_{0.01})MnSb$	-0.064	0.164	0.164	4.351	-0.01	4.518
$(Pt_{1.95}Sb_{0.05})MnSb$	-0.071	0.172	0.17	4.327	-0.005	4.522
$(Pt_{1.99}Sn_{0.01})MnSn$	-0.018	0.152	0.152	4.174	-0.027	4.319
$(Pt_{1.95}Sn_{0.05})MnSn$	-0.02	0.145	0.145	4.154	-0.027	4.283

Consequently, the energy difference ΔE between the FM and DLM states is calculated, which is the karnel parameter to estimate TC. The expression $TC=(2\Delta E)/(3k_B)$ is used to estimate the critical temperature of the Heusler compounds, where k_B is the Boltzmann constant. The estimated TC with the available experimental values. Hames and Crangle have reported the experimental TC for the PtMnSb to be 575 K and 330 K for the PtMnSn, which are closer to the values of the present calculation.

The MFA often overestimates TC in comparison to the experimental results, whereas the estimated TC for PtMnSn is in good agreement with the experiments. The reason behind the overestimation is that the framework of MFA does not include abruptness of spin within the compounds. However, the Rusz group have reported that the TC for NiMnSb to be as high as 1106 K. Their calculation closely concur with the presented result for the same compound. In addition, the estimated TC of the compounds AMnZ (x=1, y=0) is found higher than the RT (Figures 5-8) [19].

Figure 5. The solid curves indicate the total DOS of (Ni0.99Sb0.01)MnSb with 1% and 5% antisite doping of Sb atom. Vertical dashed lines are the fermi energy level. Note: ▬ top up ▬ top down.

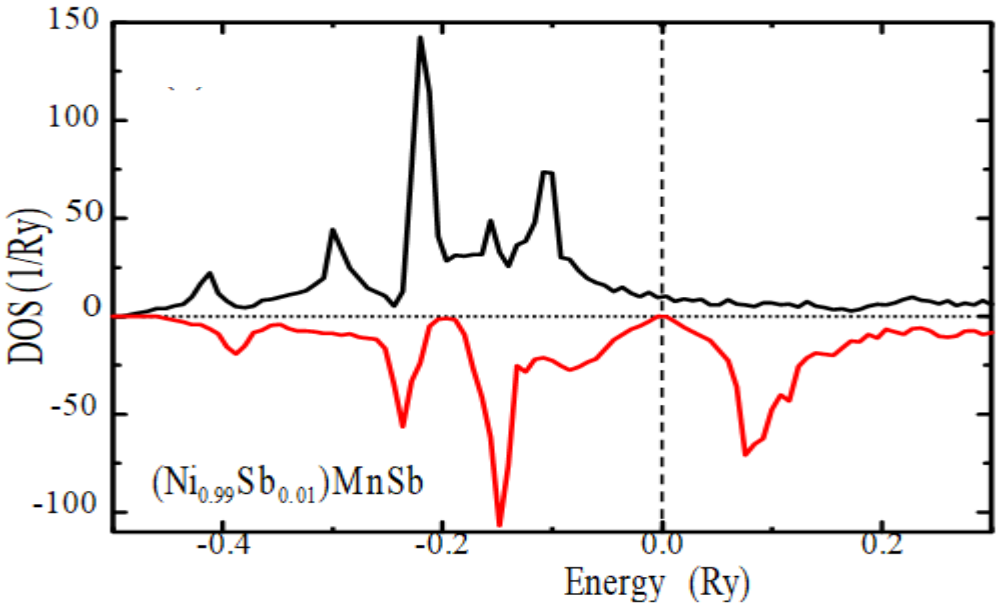

Figure 6. The solid curves indicate the total DOS of (Ni0.95Sb0.05)MnSb with 1% and 5% antisite doping of Sb atom. Vertical dashed lines are the fermi energy level. Note: top up top down.

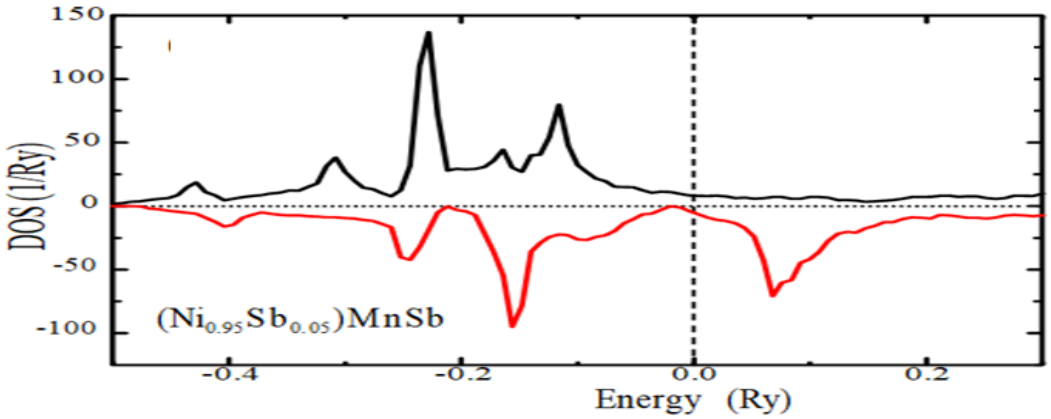

Figure 7. The solid curves indicate the total DOS of (Pd0.99Sb0.01)MnSb with 1% and 5% antisite doping of Sb atom. Vertical dashed lines are the fermi energy level. Note: top up top down.

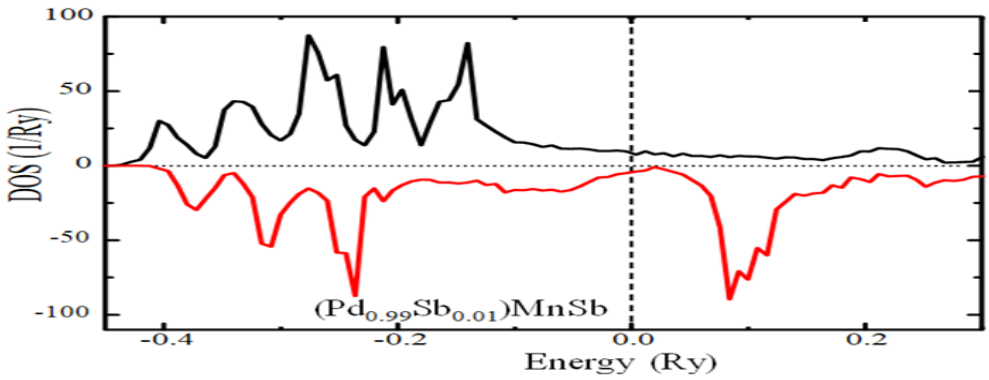

Figure 8. The solid curves indicate the total DOS of (Pd0.95Sb0.05)MnSb with 1% and 5% antisite doping of Sb atom. Vertical dashed lines are the fermi energy level. Note: top up top down.

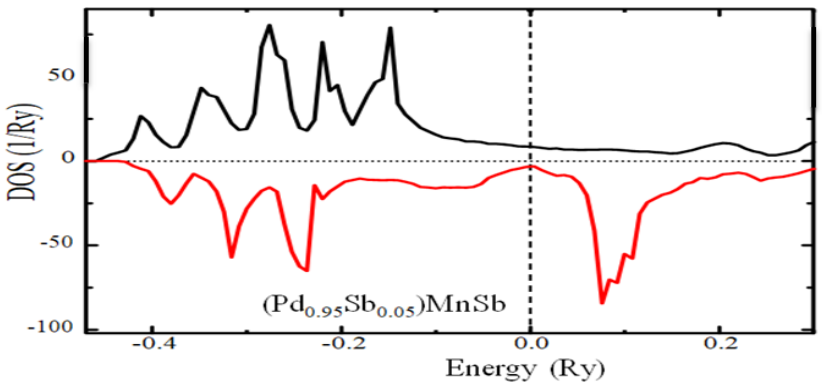

Moreover, the estimated TC with the available experimental results for the FH compounds Ni_2MnSb and Pd_2MnSb. For these two compounds, the TC is found to be higher than the RT. There was no experimental TC available for the compounds Pt_2MnSb and Pt_2MnSn. Using the MFA, Rusz have reported that the TC for Ni_2MnSb to be 575 K.

Noticed that both the Pt content compounds exhibit a low TC. Furthermore, it was assumed that the energy difference ΔE for a FH compound might be half of its HH counterpart. It is clear that this assumption is true at least approximately. However, one exception is noted for the case of Pt_2MnSb, which exhibits a quite smaller quantity. The underlying reason for this anomaly is that the partial moments of atoms are collinear with same strength and arises basically from the two unoccupied minority conduction bands. Therefore, the two A atoms together have a sum moment of about 0.25 μ_B. In contrast to this, the sp atom has a very small negative moment (-0.008 μ_B) which is quite smaller in magnitude and oppositely oriented to the spin moments of A atoms. The negative sign of the induced moment of primary group atom, belong to the fifth row of the Periodic Table, is an exceptional characteristics of the Heusler compounds (Figures 9-12) [20].

Spin resolved electronic density of states

Figure 9. The solid curves indicate the total DOS of (Pt0.99Sb0.01)MnSb, with 1% and 5% antisite doping of Sb and Sn atoms. Vertical dashed lines are the fermi energy level. Note: ▬ top up ▬ top down.

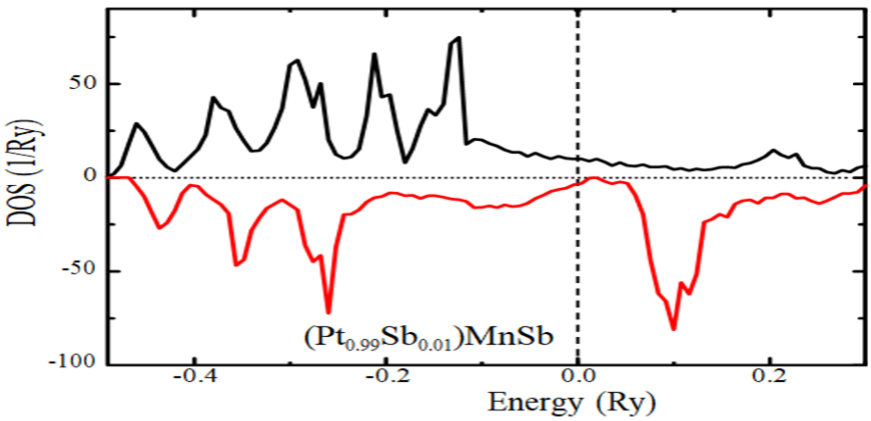

Figure 10. The solid curves indicate the total DOS of (Pt0.95Sb0.05)MnSb with 1% and 5% antisite doping of Sb and Sn atoms. Vertical dashed lines are the fermi energy level. Note: ▬ top up ▬ top down.

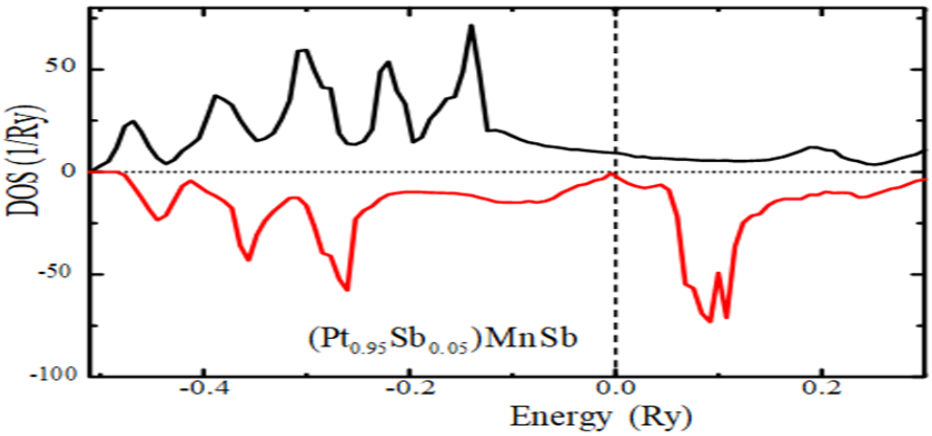

Figure 11. The solid curves indicate the total DOS of (Pt0.99Sn0.01)MnSn, with 1% and 5% antisite doping of Sb and Sn atoms. Vertical dashed lines are the Fermi energy level. Note: ▬ top up ▬ top down.

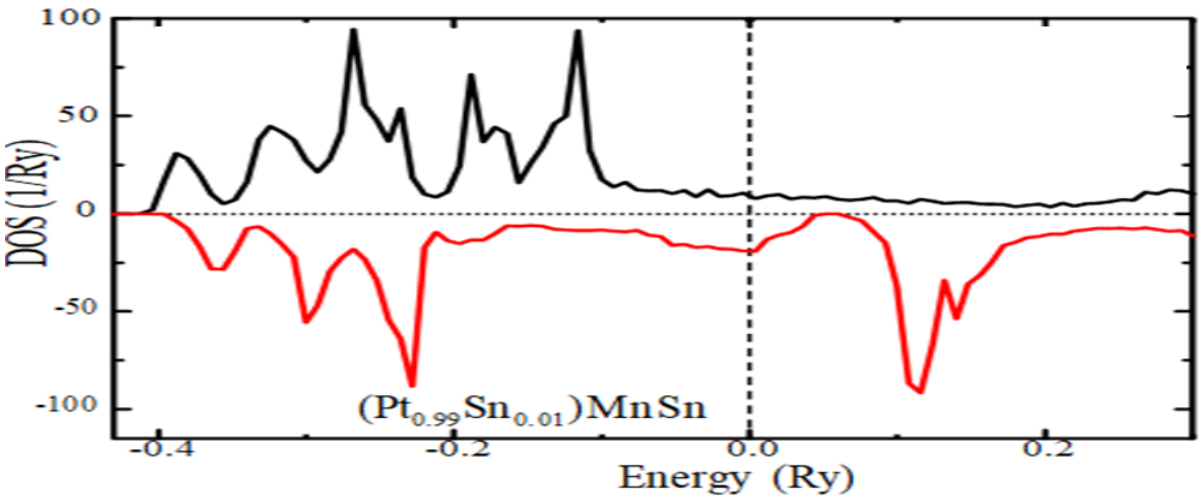

Figure 12. The solid curves indicate the total DOS of (Pt0.95Sn0.05)MnSn with 1% and 5% antisite doping of Sb and Sn atoms. Vertical dashed lines are the Fermi energy level. Note: ▬ top up ▬ top down.

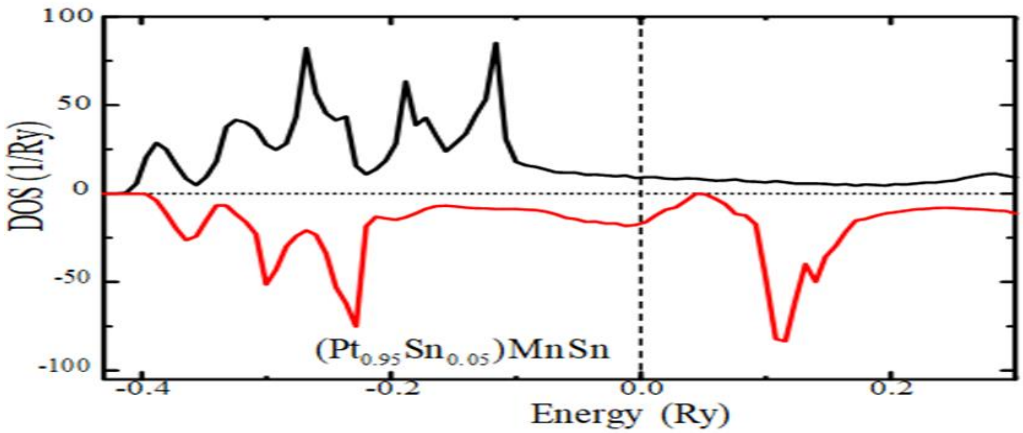

Moreover, the estimated TC with the available experimental results for the FH compounds Ni_2MnSb and Pd_2MnSb, for these two compounds, the TC is found to be higher than the RT. There was no experimental TC available for the compounds Pt_2MnSb and Pt_2MnSn. Using the MFA, the TC for Ni_2MnSb to be 575 K and reported its value to be 352 K. The DOS of a system is described by the number of spin states per an interval of occupied or empty energy levels [E, E+dE]. Its quality requires very fine k-meshes of the irreducible part of the BZ, where 328 k points were used for the calculation of DOS.

Henceforth, the spin resolved electronic DOS of the HH type compounds $(A_{1-y}Z_y)MnZ$. The KKR-Green's function calculation manifests that only $(Ni_{1-y}Sby)MnSb$ was found to be half metallic which is reported in the literature for NiMnSb with augmented spherical wave method. In $(Ni_{1-y}Sb_y)MnSb$, the Mn site has only its majority bands occupied leaving the minority bands unfilled, whereas Ni has its both bands filled. This phenomena gives rise to the

half metallic behavior of $(Ni_{1-y}Sb_y)MnSb$ with full spin polarization at the majority band and a zero DOS (no states are occupied at that energy level) at the minority band. However, on the same footing, $(Pd_{1-y}Sb_y)MnSb$, $(Pt_{1-y}Sb_y)MnSb$ and $(Pt_{1-y}Sn_y)MnSn$ might show half-metallic property. But in these compounds, in contrast to available theoretical predictions, we have found them to be FM rather than half metallic. Still these materials have high value of spin polarization at the Fermi level. Due to the higher concentrations of antisite doping, spin states are prominently shifted towards the valence band and the resulting polarization is FM (Figures 13-20).

Figure 13. The solid curves indicate the total DOS of (Ni1.99Sb0.01)MnSb, with 1% and 5% antisite doping of Sb atom. Vertical dashed lines are the Fermi energy level. Note: ▬ top up ▬ top down.

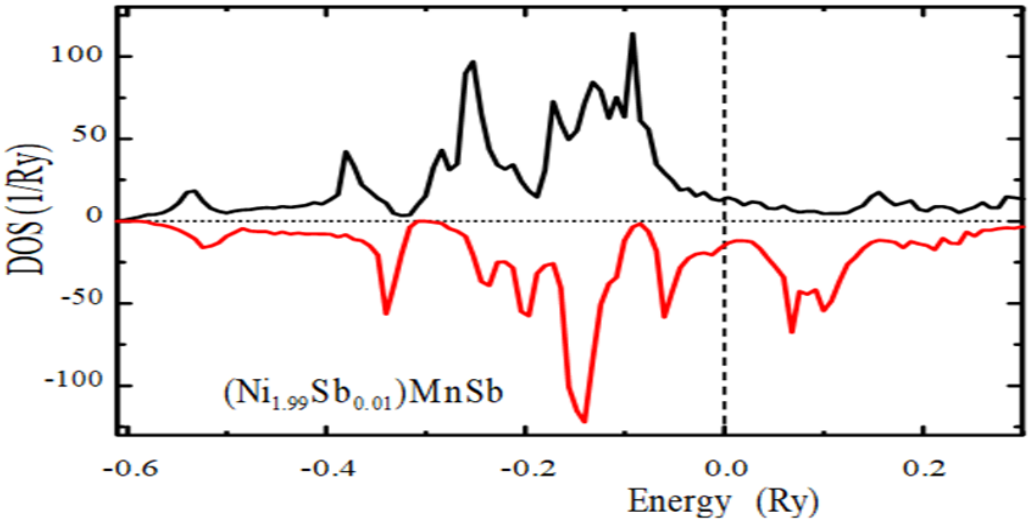

Figure 14. The solid curves indicate the total DOS of (Ni1.95Sb0.05)MnSb, with 1% and 5% antisite doping of Sb atom. Vertical dashed lines are the Fermi energy level. Note: ▬ top up ▬ top down.

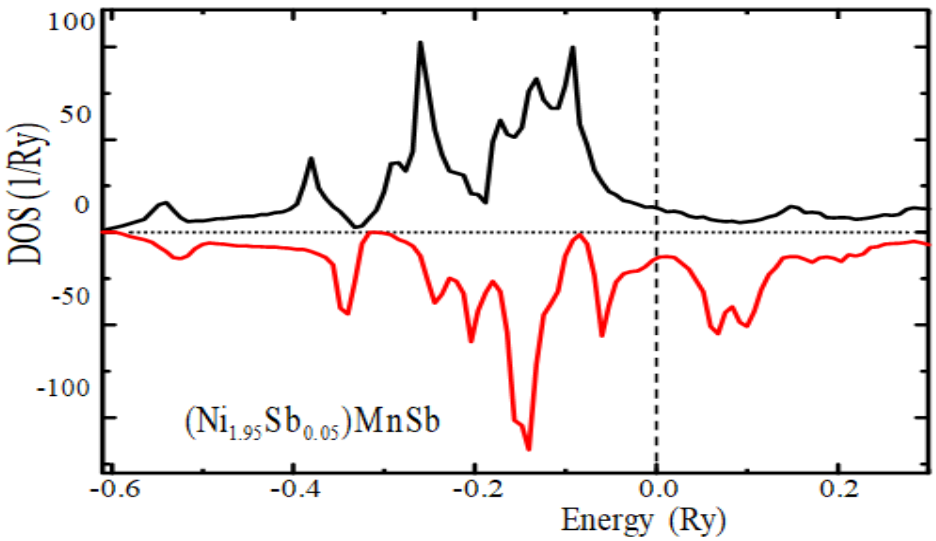

Figure 15. The solid curves indicate the total DOS of (Pd1.99Sb0.01)MnSb, with 1% and 5% antisite doping of Sb atom. Vertical dashed lines are the Fermi energy level. Note: top up top down.

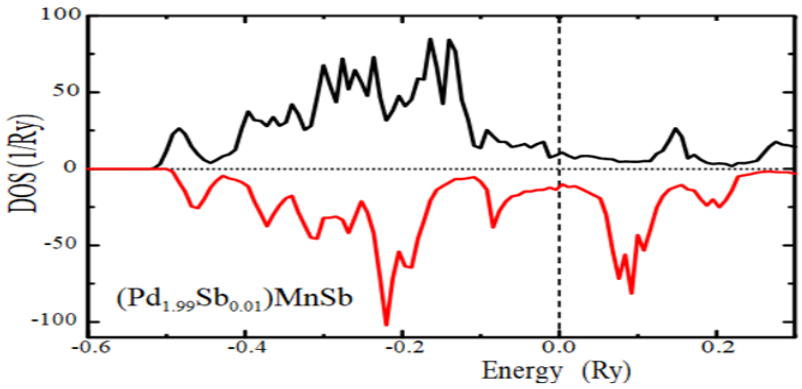

Figure 16. The solid curves indicate the total DOS of (Pd1.95Sb0.05)MnSb with 1% and 5% antisite doping of Sb atom. Vertical dashed lines are the Fermi energy level. Note: top up top down.

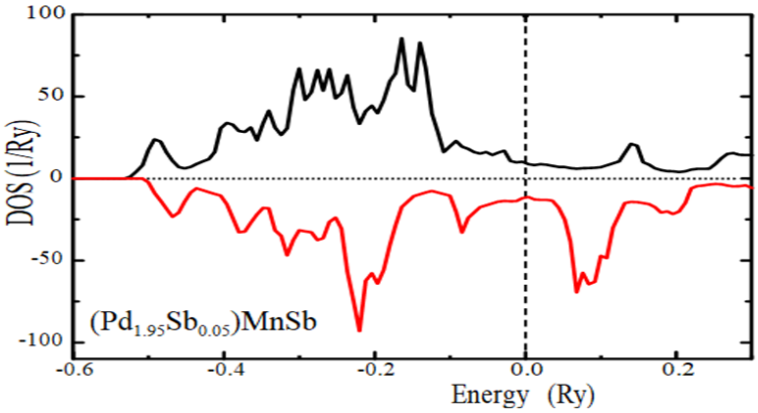

Figure 17. The solid curves indicate the total DOS of (Pt1.99Sb0.01)MnSb, with 1% and 5% antisite doping of Sb and Sn atoms. Vertical dashed lines are the Fermi energy level. Note: top up top down.

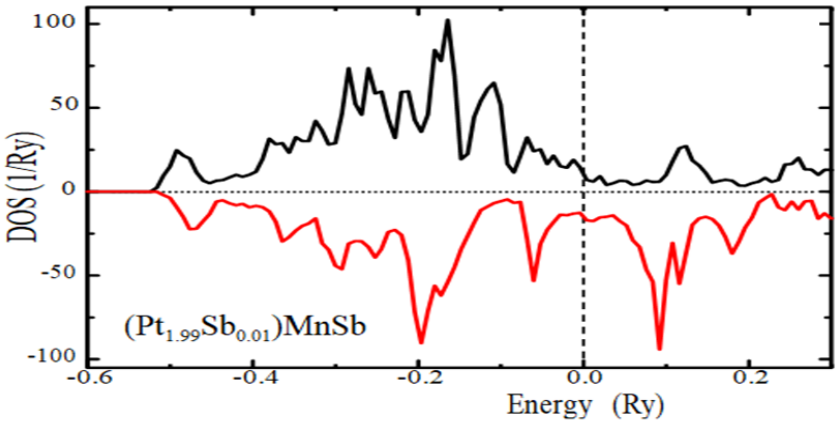

Figure 18. The solid curves indicate the total DOS of (Pt1.95Sb0.05)MnSb, with 1% and 5% antisite doping of Sb and Sn atoms. Vertical dashed lines are the Fermi energy level. Note: ▬ top up ▬ top down.

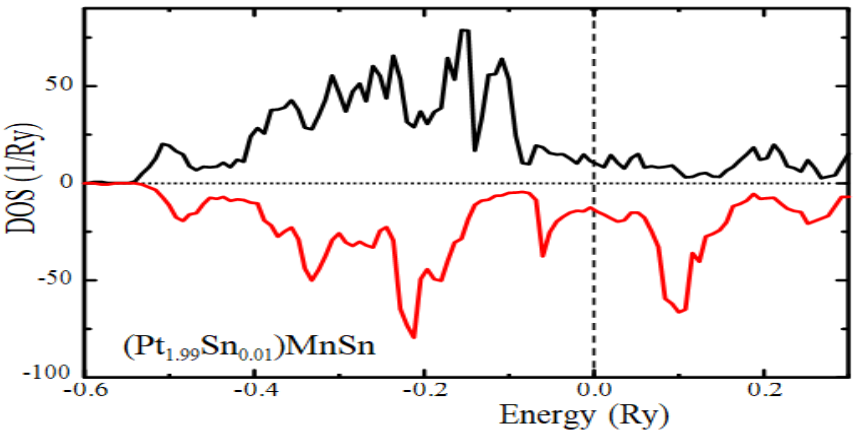

Figure 19. The solid curves indicate the total DOS of (Pt1.99Sn0.01)MnSn, with 1% and 5% antisite doping of Sb and Sn atoms. Vertical dashed lines are the Fermi energy level. Note: ▬ top up ▬ top down.

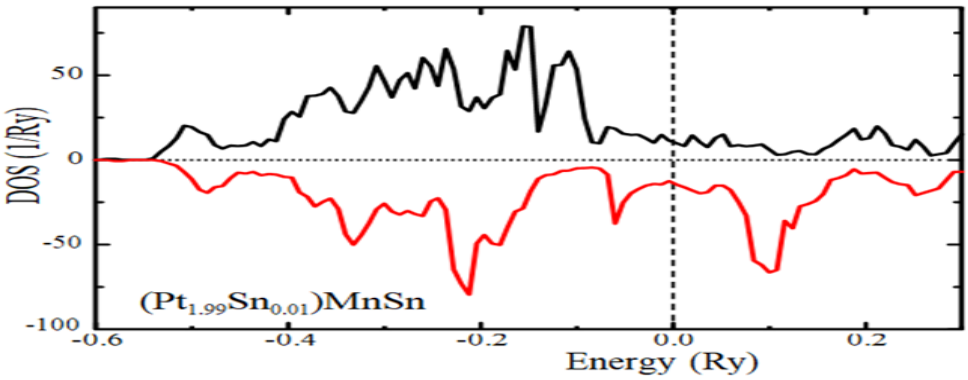

Figure 20. The solid curves indicate the total DOS of (Pt1.95Sn0.05)MnSn with 1% and 5% antisite doping of Sb and Sn atoms. Vertical dashed lines are the Fermi energy level. Note: ▬ top up ▬ top down.

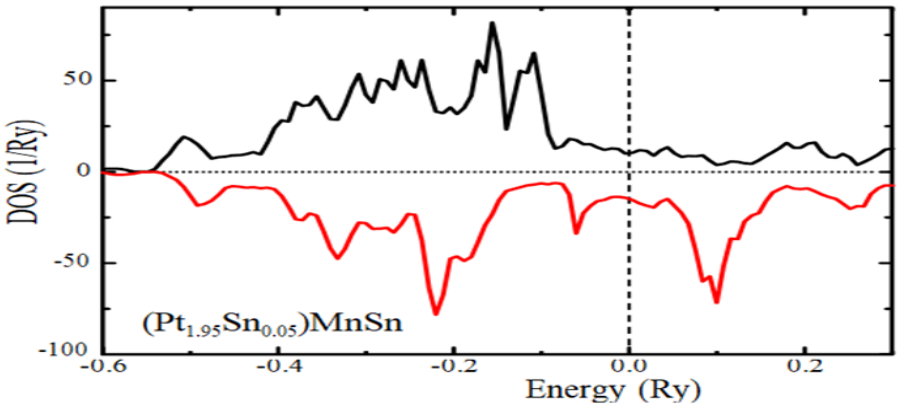

The spin resolved DOS of the FH type compounds ($A_{2-y}Z_y$) MnZ are gathered. The DOS, a function of energy inverse, is a continuous pattern of resoluted electronic states in metal due to the presence of local potential, whereas the pattern discontinuity arises in half-metal. The total DOS by solid curves are plotted together in the figures. The valence band extends around the Fermi level and the spin-split DOS shows a large peak below the Fermi level for these compounds. In the case of FH type compounds, each Mn atom has eight A atoms as first neighbors instead of four as in the case of HH type compounds ($A_{1-y}Z_y$) MnZ. Therefore, the hybridization effect is very important decreasing even further the Mn spin moment to less than 4 μB in the case of the compounds ($Ni_{2-y}Sb_y$)MnSb. The spin moments of A atoms are ferromagnetically coupled to the Mn spin moment and the materials possess a high spin polarization of the electron states at the Fermi level. The higher antisite doping produces more antisit moment and shifting of states, lying deep in energy, stabilizes the FM state [21].

CONCLUSION

Spin polarization and collinear magnetic properties have been investigated for Heusler type compounds ($A_{2-x-y}Z_y$) MnZ, using the KKR-Green's funtion approach, where the wave functions and charge densities are constructed by spherically symmetric atomic sphere potentials. Extensive calculations show a large magnetic effects of Mn atom of the compounds. The magnetic moments are compared with the available experimental values, where the observed moments highly support the calculated results. The estimated values of TC for the Heusler compounds are found higher than the RT, whereas only two of the four FH compounds exhibit low TC. The TC is related proportionally to the spin density wave, that is, the higher spin density produces more TC. The ($Ni_{1-y}Sb_y$)MnSb with 1% antisite doping retain the full spin polarized charge injection in the spintronic devices. The novel functional devices that control electrons and spins are considered candidates to be fabricated by the emergent magnetic materials.

ACKNOWLEDGMENT

The present work was performed with the advanced computational facilities provided by the Center For Advanced Research In Sciences (CARS), University of Dhaka. The authors are thankful to CARS for the supports.

REFERENCES

1. Webster PJ. Heusler alloys. Cont Phy. 1969;10:559-577.
2. Campbell CC. Hyperfine field systematics in Heusler alloys. J Phys F Metal Phys. 1975;5:1931.
3. Kulkova SE, et al. The electronic structure and magnetic properties of full-and half-Heusler alloys. Mat Trans. 2006;47:599-606.
4. Heusler F. Uber magnetische manganlegierungen. Verh Dtsch Phys Ges. 1903;5:219.
5. De Groot RA, et al. New class of materials: Half-metallic ferromagnets. Phys Rev Letters. 1983;50:2024.
6. Rusz J, et al. Exchange interactions and curie temperatures in Ni_{2-x} Mn Sb alloys. First Prin Stdy. 2006;73:214412.
7. Groot RD, et al. Half-metallic ferromagnets and their magneto-optical properties. J App Phys. 1984;55:2151-2154.
8. Kaneko T, et al. Pressure effect on the curie point of the Heusler alloys Ni_2MnSn and Ni_2MnSb. J App Phy. 1981;52:2046-2048.
9. Hirohata A, et al. Heusler alloy/semiconductor hybrid structures. Cur Opi Solid State Mat Sci. 2006;10:93-107.
10. Skomski R, et al. Indirect exchange in dilute magnetic semiconductors. J App Phy. 2006;99:08D504.
11. Casula F, et al. Generalized muffin-tin orbitals for electronic structure studies of surfaces, interfaces, and organic solids. J Chem Phys. 1983;78:858-875.

12. Offernes L, et al. Prediction of composition for stable half-Heusler phases from electronic-band-structure analyses. J Alloys Comp. 2008;30:47-60.
13. Endo K. Magnetic studies of Cl b-Compounds CuMnSb, PdMnSb and Cu_{1-x} (Ni or Pd) x MnSb. J Phy Soc Japan. 1970;29:643-649.
14. Masumoto H, et al. Magnetic properties of Clb-type pseudo-ternary intermetallic compounds Pt_{1-x} AuxMnSb. Tran Japan Ins Mtls. 1976:588-591.
15. Hames FA, et al. Ferromagnetism in Heusler-type alloys based on platinum-group or palladium-group metals. J App Phy. 1971;15:1336-1338.
16. Hames FA. Ferromagnetic-alloy phases near the compositions Ni_2 MnIn, Ni_2 MnGa, Co_2 MnGa, Pd_2 MnSb and PdMnSb. J App Phy. 1960;S370-371.
17. Webster PJ, et al. Magnetic and chemical order in Pd_2 MnAl in relation to order in the Heusler alloys Pd_2 MnIn, Pd_2 MnSn, and Pd_2 MnSb. J App Phy. 1968;1:471-473.
18. Roy T, et al. Ab initio study of effect of Co substitution on the magnetic properties of Ni and Pt-based Heusler alloys. Phys Let A. 2017;25:1449-1456.
19. Akai H, et al. L-edge resonant magneto-optical Kerr effect of a buried Fe nanofilm. Phys Rev B. 2017; 30:134432.
20. Galanakis I, et al. Spin-polarization and electronic properties of half-metallic Heusler alloys calculated from first principles. J Phys Cond Mat. 2007;3:315213.
21. Galanakis I, et al. Origin and properties of the gap in the half-ferromagnetic Heusler alloys. Phys Rev B. 2002;66:134428.